THE JOURNAL OF BIOLOGICAL CHEMISTRY VOL. 282, NO. 5, pp. 3312–3324, February 2, 2007

Cochlear Function in Mice Lacking the BK Channel α, β1, or β4 Subunits*[S]

Received for publication, September 11, 2006, and in revised form, November 21, 2006 Published, JBC Papers in Press, November 29, 2006, DOI 10.1074/jbc.M608726200

Sonja J. Pyott[‡1], Andrea L. Meredith[§], Anthony A. Fodor[¶], Ana E. Vázquez[‖], Ebenezer N. Yamoah[‖], and Richard W. Aldrich[**]

From the [‡]Department of Otolaryngology Head and Neck Surgery, The Johns Hopkins School of Medicine, Baltimore, Maryland 21205, the [§]Department of Physiology, University of Maryland School of Medicine, Baltimore, Maryland 21201, the [¶]Department of Bioinformatics/Computer Science, University of North Carolina, Charlotte, North Carolina 28233, the [‖]Center for Neuroscience, Department of Otolaryngology, University of California, Davis, California 95616-8635, and the [**]Section of Neurobiology, University of Texas, Austin, Texas 78712

Large conductance voltage- and calcium-activated potassium (BK) channels are important for regulating many essential cellular functions, from neuronal action potential shape and firing rate to smooth muscle contractility. In amphibians, reptiles, and birds, BK channels mediate the intrinsic frequency tuning of the cochlear hair cell by an electrical resonance mechanism. In contrast, inner hair cells of the mammalian cochlea are extrinsically tuned by accessory structures of the cochlea. Nevertheless, BK channels are present in inner hair cells and encode a fast activating outward current. To understand the role of the BK channel α and β subunits in mammalian inner hair cells, we analyzed the morphology, physiology, and function of these cells from mice lacking the BK channel α (*Slo*$^{-/-}$) and also the β1 and β4 subunits (β1/4$^{-/-}$). β1/4$^{-/-}$ mice showed normal subcellular localization, developmental acquisition, and expression of BK channels. β1/4$^{-/-}$ mice showed normal cochlear function as indicated by normal auditory brainstem responses and distortion product otoacoustic emissions. *Slo*$^{-/-}$ mice also showed normal cochlear function despite the absence of the BKα subunit and the absence of fast activating outward current from the inner hair cells. Moreover, microarray analyses revealed no compensatory changes in transcripts encoding ion channels or transporters in the cochlea from *Slo*$^{-/-}$ mice. *Slo*$^{-/-}$ mice did, however, show increased resistance to noise-induced hearing loss. These findings reveal the fundamentally different contribution of BK channels to nonmammalian and mammalian hearing and suggest that BK channels should be considered a target in the prevention of noise-induced hearing loss.

BK channels regulate many functions, from neuronal action potential shape (1–3) and firing rate (4, 5) to smooth muscle contractility (6–8). In amphibians, reptiles, and birds, BK channels mediate the intrinsic frequency selectivity of the cochlear hair cell (9). BK channels are composed of four α pore-forming subunits (10). Regulatory β subunits (β1–4) have also been identified (11–15). In nonmammalian hair cells, β subunits may associate with the BKα subunit to shape the resonant frequency (16).

Numerous studies have shown that BK channels are also present in inner hair cells (IHCs),[2] the subset of hair cells in the mammalian cochlea responsible for transducing sound to the central nervous system. IHCs express a potassium current (termed $I_{K,f}$) pharmacologically similar to BK currents, showing sensitivity to low concentrations of tetraethylammonium, charybdotoxin, and iberiotoxin (17–21). The transcript for the BKα subunit has been detected in IHCs (22, 23), and immunostaining has verified expression of the BKα subunit in IHCs (17, 20, 21, 24). Additionally, transcripts for both the BKβ1 and β4 subunit have been identified in IHCs (22).

The exact function of BK channels in IHCs is unknown and likely to be different from that in nonmammalian hair cells. Unlike nonmammalian hair cells, IHCs are extrinsically tuned by accessory structures of the cochlea (9), the BK current found in IHCs does not require external calcium for activation (18, 25, 26), and BK channels in IHCs are extrasynaptic (20). Nevertheless, the importance of BK channels for the expression of mammalian hearing has been suggested indirectly in mice: $I_{K,f}$ becomes expressed in mouse IHCs at the onset of hearing (approximately 2 weeks postnatal (19)), and mice lacking the thyroid hormone receptor β show delayed acquisition of $I_{K,f}$ by the IHCs and dramatically elevated auditory thresholds (27).

To assess directly the contribution of the BKα and BKβ subunits to mammalian hearing, we analyzed the morphology, physiology, and function of IHCs cells from mice lacking the BKα subunit (*Slo*$^{-/-}$) and the BKβ1 and BKβ4 subunits (β1/4$^{-/-}$). We found normal cochlear function in both *Slo*$^{-/-}$ and β1/4$^{-/-}$ mice. *Slo*$^{-/-}$ mice, however, showed increased resistance to noise-induced hearing loss (NIHL). These findings

* This work was supported by National Institutes of Health Grants DC07592 and DC03828 (to E. N. Y.), a National Science Foundation graduate research fellowship (to S. J. P.), and the Mathers Foundation (to R. W. A.). The costs of publication of this article were defrayed in part by the payment of page charges. This article must therefore be hereby marked "*advertisement*" in accordance with 18 U.S.C. Section 1734 solely to indicate this fact.

[S] The on-line version of this article (available at http://www.jbc.org) contains supplemental Fig. S1.

[1] To whom correspondence should be addressed: Dept. of Otolaryngology Head and Neck Surgery, Johns Hopkins School of Medicine, 720 Rutland Ave., Traylor 521, Baltimore, MD 21205. Tel.: 410-955-3877; Fax: 410-614-4748; E-mail: spyott@jhmi.edu.

[2] The abbreviations used are: IHC, inner hair cell; NIHL, noise-induced hearing loss; ABR, auditory brainstem response; DPOAE, distortion product otoacoustic emission; PBS, phosphate-buffered saline; NF200, neurofilament-200; IBTX, iberiotoxin; OBN, octave band noise; TS, threshold shift; OHC, outer hair cell; WT, wild type; GM, geometric mean; NF, noise floor; dB, decibel(s); SPL, sound pressure level.

reveal the fundamentally different contribution of BK channels to nonmammalian and mammalian hearing and suggest that BK channels may be an important target in the prevention of NIHL.

EXPERIMENTAL PROCEDURES

Generation of Transgenic Mice—$Slo^{-/-}$ were generated as described previously (7) and maintained on an inbred FVB/NJ background. All results shown are for $Slo^{+/+}$, $Slo^{+/-}$, and $Slo^{-/-}$ littermates. $\beta1^{-/-}$ mice were generated as described previously (6) and maintained on an inbred C57BL/6 background. $\beta4^{-/-}$ mice were generated as described previously (28). $\beta1/4^{-/-}$ double transgenic mice were generated by breeding inbred $\beta1^{-/-}$ with outbred $\beta4^{-/-}$ mice. All genotypes were verified by PCR on genomic tail DNA. Because $\beta4^{-/-}$ mice were on a mixed background, experiments involving electrophysiology, auditory brainstem response (ABR) measurements, and distortion product otoacoustic emission (DPOAE) measurements were also performed on wild type 129X1/SvJ mice, although only data from wild type C57BL/6 (C57 WT) mice are shown. No differences were detected between $\beta1/4^{-/-}$ and C57 WT mice with electrophysiology, ABR, or DPOAE. No differences were detected between $\beta1/4^{-/-}$ and wild type 129X1/SvJ with electrophysiology or ABR. $\beta1/4^{-/-}$ did have significantly greater magnitude DPOAEs compared with wild type 129X1/SvJ (although noise floors were similar). However, because $\beta1/4^{-/-}$ mice are genetically more similar to C57 WT mice and because 129X1/SvJ mice are known to have large variations in the magnitudes of their DPOAEs (29), this finding was not investigated further.

Immunostaining and Confocal Microscopy—Whole cochleae were dissected from mice and immediately perfused through the round window with 4% paraformaldehyde in phosphate-buffered saline (PBS) at pH 7.4. Cochleae were fixed in 4% paraformaldehyde/PBS for 2 h at 4 °C before being rinsed with PBS. Apical turns of the organs of Corti were excised from the cochleae and blocked in blocking buffer (PBS with 5% normal goat serum and 0.2% Triton X-100) for 2 h at room temperature. Turns were incubated in the primary antibody diluted in blocking buffer overnight at 4 °C, rinsed 3 times for 20 min each in PBT (PBS with 0.2% Triton X-100), incubated in the secondary antibody diluted in blocking buffer for 4 h at room temperature, rinsed 3 times for 20 min each in PBT, and rinsed in PBS before mounting on glass slides in Vectashield mounting medium (Vector Laboratories, Burlingame, CA). All incubations and rinses were performed on a rocking table.

The mouse monoclonal antibody against the BKα subunit was graciously provided by Dr. James S. Trimmer (University of California, Davis) and used at a final concentration of 10 μg/ml as described previously (20). The rabbit polyclonal antibody against the BKα subunit (APC-021) was purchased from Alomone Laboratories (Jerusalem, Israel) and diluted 1:500. The monoclonal antibody against calretinin (diluted 1:1000), the polyclonal antibody against synapsin (diluted 1:300), and the polyclonal antibody against neurofilament-200 (NF200; diluted 1:200) were purchased from Chemicon (Temecula, CA). The monoclonal antibody against NF200 was graciously provided by Novocastra Laboratories (Newcastle upon Tyne, UK) and diluted 1:50. Fluorescein isothiocyanate-conjugated phalloidin (diluted 1:100) was purchased from Molecular Probes, Inc. (Eugene, OR) and provided graciously by Dr. W. James Nelson (Stanford University). Secondary antibodies (Alexa Fluor 488, 594, and 633) were purchased from Molecular Probes and diluted 1:1000.

Simultaneous one- or two-color fluorescence images were acquired on a Leica confocal SP2 AOBS (Leica Microsystems, Bannockburn, IL) with a 63× oil immersion Leica HCX PL APO objective (numerical aperture = 1.4). Z-stacks (~70 optical sections) were collected at 0.3 μm. Optical sections were combined, and three-dimensional reconstructions were performed through volume rendering using Volocity 2.0.1 (Improvision, Lexington, MA).

Electrophysiology—Apical turns of the organ of Corti were excised from mice and used within 1 h of the dissection. Extracellular solution contained 155 mM NaCl, 5.8 mM KCl, 0.9 mM $MgCl_2$, 1.3 mM $CaCl_2$, 0.7 mM NaH_2PO_4, 5.6 mM D-glucose, and 10 mM HEPES at pH 7.4. For indicated experiments, 100 nM iberiotoxin (IBTX; Tocris Cookson, Bristol, UK) was added to the extracellular solution and delivered locally via a gravity flow pipette. Pipette solution contained 150 mM KCl, 3.5 mM $MgCl_2$, 5 mM EGTA, 5 mM HEPES, and 2.5 mM Na_2ATP, pH 7.2. Recording electrodes were pulled from micropipettes (VWR Scientific, West Chester, PA) and coated with wax (KERR sticky wax, Romulus, MI) to minimize electrode capacitance. Pipette resistances in solution were 2–3 megaohms. Total series resistances (at most 5 megaohms) were compensated 70% on-line. The indicated test potentials are not corrected for liquid junction potentials (calculated to be ~4 mV) or for the voltage drop across the remaining uncompensated series resistance (at most 1.5 megaohms). Experiments were done at room temperature. Data were acquired with an Axopatch 200A amplifier (Axon Instruments, Foster City, CA), filtered at 10 kHz, and digitized at 50 kHz with a 16 bit A/D converter (InstruTech ITC-16; InstruTech, Port Washington, NY) under the control of pulse acquisition software (HEKA). All traces shown and used for analyses are averaged from at least five recordings. Analyses were performed with Igor Pro (Wavemetrics, Lake Oswego, OR) and Microsoft Excel.

ABR Measurements—Mice were anesthetized with ketamine (80 mg/kg) and xylazine (20 mg/kg) by intraperitoneal injection. To record electrical potentials, the mouse was placed onto a 37 °C heating pad, and subdermal silver wire electrodes were inserted at the vertex (reference), ventrolateral to the measured ear (active), and at the back of the animal (ground). Electrical signals were then recorded in response to a 25-μs click (broadband) or pip (single frequency) sound stimuli presented to one ear from each mouse. Electrical signals were averaged (from at least 200 repetitions) and were collected from 10 to 100 dB SPL in 5–10-dB steps. Thresholds were defined as the sound pressure level where a stimulus-correlated response was clearly identified in the recorded signal.

DPOAE Measurements—Mice were anesthetized as described above. DPOAEs were measured as described previously (30). The f1 and f2 primary tones were generated by a dual channel synthesizer (Hewlett-Packard 3326A) and attenuated using custom software that operated a digital signal processor

on board a personal computer system. The f1 and f2 primaries (f2/f1 = 1.25) were then presented over two separate ear speakers (Radio Shack, Realistic, Dual Radial Horn Tweeters) and delivered to the outer ear canal through an acoustic probe fitted with a soft rubber tip (ER3-34 Infant Silicon Tip; Etymotic Research, Elk Grove Village, IL). Ear canal sound pressure levels, measured by an emissions microphone assembly (ER-10B+; Etymotic Research) embedded in the probe, were sampled, synchronously averaged, and processed using a fast Fourier transform for geometric mean (GM) frequencies ($(f1 \times f2)^{0.5}$) ranging from 5.6 to 17.2 kHz (f2 = 6.3–19.2 kHz). Corresponding noise floors (NFs) were computed by averaging the levels of the ear canal sound pressure for five frequency bins above and below the DPOAE frequency bin. For test frequencies above 20 kHz, a computer-controlled dynamic signal analyzer (Hewlett-Packard 3561A) was used. The related NFs were estimated by averaging the levels of the ear canal sound pressure for the two fast Fourier transform frequency bins below the DPOAE frequency. NFs were not found to be significantly different between $Slo^{+/+}$, $Slo^{+/-}$, $Slo^{-/-}$ mice or between C57 WT and $\beta 1/4^{-/-}$ mice. Thus, only the group averaged NF is shown. For each genotype, the mean ± S.E. DPOAEs are presented as a function of the GM frequencies. Three GM frequencies (17.1, 18.4, and 19.7 kHz) were not included in the average plots shown due to artifacts related to the 1/4-wave cancellation effect in the mouse ear canal, which result in primary tones being more intense than their targeted levels (30).

RNA Isolation and cDNA Synthesis—In parallel experiments, total RNA was extracted from either the cochleae or cerebellum from between one and four 8-week-old $Slo^{+/+}$ and $Slo^{-/-}$ mice using TRIzol reagent (Invitrogen) according to the provided directions. Extracted RNA was further purified and concentrated using the Qiagen RNeasy Mini and Micro Kits (Qiagen; Valencia, CA) according to the manufacturer's protocol. Cochleae provided between 1 and 4 μg of total RNA; each half-cerebellum provided ~10 μg of total RNA. Total RNA yield and purity were assessed with a 2100 Bioanalyzer (Agilent Technologies, Mountain View, CA). All samples had A260/A280 ratios of 1.9–2.1 and showed two sharp peaks corresponding to the 18 and 28 S RNA on electropherograms. First strand synthesis was performed using either one-cycle or two-cycle cDNA synthesis kits (Affymetrix, Santa Clara, CA).

Microarrays—Affymetrix murine genome 430 2.0 GeneChips were processed at the Stanford University Microarray Core Facility. Each microarray contains ~45,000 probe sets that include known genes, expressed sequence tags, and internal housekeeping and control genes. After target preparation, hybridization, and signal acquisition according to standard Affymetrix protocols (available on the World Wide Web www.affymetrix.com). Data were analyzed as described previously (31). Briefly, data were normalized using dchip (available on the World Wide Web at biosun1.harvard.edu/complab/dchip/) with the default parameters. Hybridization signals for each gene were reported as the median of the 11 perfect match probes in each probe set. To compare differences in the expression of channels and transporters between the cochleae of $Slo^{+/+}$ and $Slo^{-/-}$ mice, transcripts containing the keywords "channels" and "transporters" (ignoring case) in the Annotations in the Mouse430_2.gin file provided by Affymetrix were compared.

NIHL Measurements—The octave band noise (OBN) was generated using white noise output by a USB-controlled digital signal processor system (Intelligent Hearing Systems, Miami, FL) connected to an IBM-compatible PC and filtered through a custom-made filter box (Intelligent Hearing Systems) using a four-pole band pass filter with a center frequency of 10 kHz and a bandwidth from 8 to 16 kHz. The signal was then amplified using a Crown D75A and transduced by four speakers (Radio Shack) placed in the walls of the sound chamber. The noise spectrum, analyzed with the dynamic signal analyzer in 1/3-octave frequency bands, ranged from 8 to 15 kHz, with the maximum energy of 105 dB SPL at 10 kHz.

During the 1-h OBN exposure, one mouse was placed into each compartment (12 cm wide) of a custom-made, wire mesh cage consisting of four compartments with free access to food. During each free field exposure session, a maximum of four mice, each in an individual compartment, were exposed to the OBN. The wire mesh cage was positioned in the center of the sound isolation chamber, fitted with hard reflecting surfaces that ensure homogeneous exposure levels. The homogeneity of the sound field was confirmed using a Quest sound meter with the microphone placed in various places of the cage.

One day after measuring base line ABR and DPOAE responses, mice were exposed to the 105-dB SPL stimulus for 1 h. Threshold shifts (TSs) for each genotype were determined by comparing the differences in the mean ABR and DPOAE responses measured 5 days after recovery with their prenoise-exposed values.

Statistics—Results are presented as the mean ± S.E. of the mean. Box plots are shown with the median line, whisker tops, and bottoms indicating the 90th and 10th percentile and box tops and bottoms indicating the 75th and 25th percentile. *p* values were calculated using a two-tailed paired or unpaired (as appropriate) *t* test assuming unequal variances.

RESULTS

Inner Hair Cells from $Slo^{-/-}$ Mice Do Not Express the BKα Subunit and Have Normal Morphology and Synaptic Innervation—Immunostaining with antibodies against the BK channel was performed to confirm the absence of the BKα subunit from the IHCs of $Slo^{-/-}$ mice. Fig. 1 shows organs of Corti from 8-week-old $Slo^{+/+}$ and $Slo^{-/-}$ mice double immunostained with a monoclonal antibody against the hair cell marker calretinin (*green*) and a polyclonal antibody against the BK channel (*red*). IHCs from $Slo^{+/+}$ mice show clustered expression of BK channels near the apex of the IHCs, as has been previously reported (17, 20). This pattern of expression is observed when staining with either the polyclonal (*green*) or monoclonal antibody (*red*) against the BK channel (each recognizing distinct epitopes of the BKα subunit). In contrast, IHCs from $Slo^{-/-}$ mice show no staining for BK channels in IHCs with either the polyclonal or monoclonal antibody. These data confirm the specificity of both the monoclonal and polyclonal antibodies for the BKα subunit and, more importantly, verify the absence of the BKα subunit from the IHCs from $Slo^{-/-}$ mice.

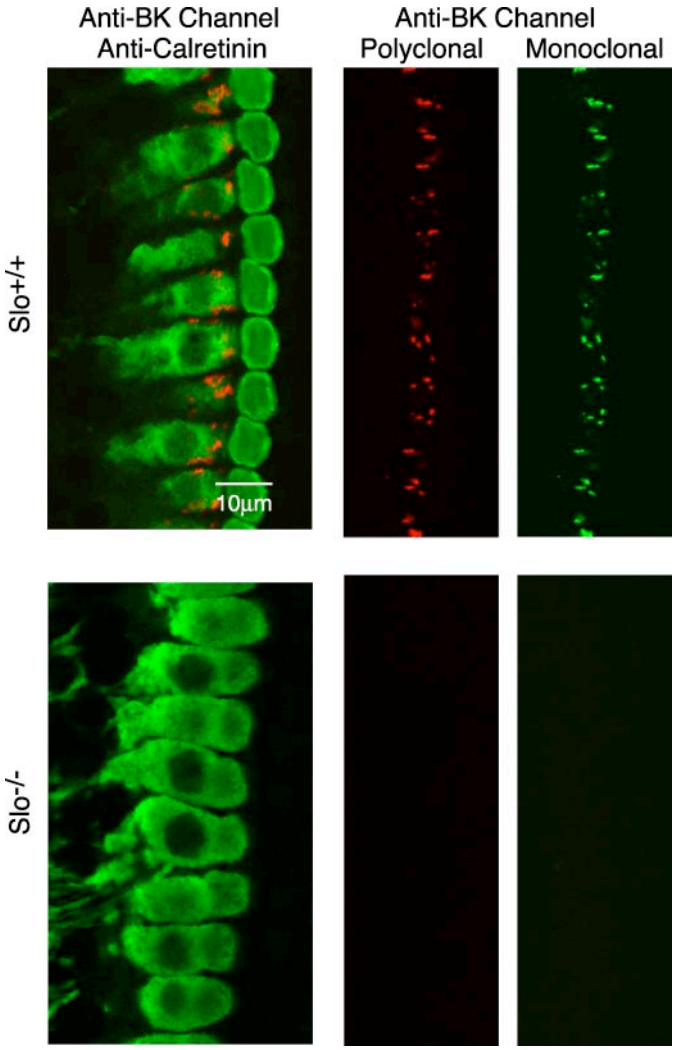

FIGURE 1. **Inner hair cells from *Slo*$^{-/-}$ mice do not express the BKα subunit.** Intact organs of Corti from 8-week-old *Slo*$^{+/+}$ and *Slo*$^{-/-}$ mice were immunostained as described under "Experimental Procedures." Immunostaining with a monoclonal calretinin antibody (*green*) and polyclonal BK channel antibody (*red*) shows the presence of punctate staining for BK channels in IHCs from *Slo*$^{+/+}$ mice and the absence of BK channels in IHCs from *Slo*$^{-/-}$ mice. Immunoreactivity for BK channels is seen in IHCs from *Slo*$^{+/+}$ mice and absent from IHCs from *Slo*$^{-/-}$ mice when staining with either a polyclonal (*green*) or monoclonal (*red*) antibody against the BK channel.

Because mice with hearing deficits arising from the genetic deletion of ion channels can show hair cell degeneration (32–34) or otherwise abnormal innervation (35), organs of Corti excised from 8-week-old *Slo*$^{+/+}$ and *Slo*$^{-/-}$ mice were immunostained to assess the morphology and synaptic architecture of the IHCs (Fig. 2). Immunostaining with either a polyclonal or monoclonal (data not shown) antibody against calretinin, an endogenous calcium buffer enriched in the sensory hair cells (36), shows that the IHCs from *Slo*$^{-/-}$ mice are intact and normally arranged compared with those from *Slo*$^{+/+}$ mice. To assess the afferent innervation to the IHCs, organs of Corti were immunostained with an antibody against NF200, a known marker of afferent fibers in the organ of Corti (37). No gross differences in the arrangement or density of the afferent nerve fibers to the IHCs were observed between *Slo*$^{+/+}$ and *Slo*$^{-/-}$ mice across replicates (Fig. 2). Efferent innervation was assessed by staining for synapsin, a synaptic vesicle marker expressed only in the conventional (nonribbon) efferent synapses of the organ of Corti (38). Synapsin staining revealed no consistent differences in the arrangement or density of the efferent innervation of the OHCs and IHC afferent terminals between *Slo*$^{+/+}$ and *Slo*$^{-/-}$ mice across replicates (Fig. 2).

Inner Hair Cells from Slo$^{-/-}$ *Mice Lack the Fast Activating BK Current and Have No Compensatory Changes in the Remaining Outward Currents*—IHCs from mice express potassium currents that can be distinguished by their relative rates of activation. The fast activating component is carried by BK channels, whereas the slowly activating current is most likely carried by a composite of channels (17, 19, 20, 39–41). Whole cell voltage clamp recordings were performed on IHCs from organs of Corti excised from 3-week-old *Slo*$^{+/+}$, *Slo*$^{+/-}$, and *Slo*$^{-/-}$ mice to examine the contributions of both the fast and slowly activating currents. The IHCs from both *Slo*$^{+/+}$ and *Slo*$^{+/-}$ show fast activating potassium currents (Fig. 3*A*) that have been described previously (19). This component can be blocked by applying 100 nM IBTX (Fig. 3*B*) to the external solution. The known specificity of IBTX for the BK channel (42) verifies that this current is carried by the BK channel. Interestingly, IHCs from *Slo*$^{+/-}$ mice show levels of BK current comparable with those isolated from the IHCs of *Slo*$^{+/+}$ mice (Fig. 3*C*). Importantly, *Slo*$^{-/-}$ mice show no fast activating potassium current (Fig. 3*A*), and the application of 100 nM IBTX has no effect on the remaining currents (Fig. 3*B*). The inability to isolate an IBTX-sensitive current from *Slo*$^{-/-}$ mice (Fig. 3*C*) provides definitive evidence that the fast activating, IBTX-sensitive current seen in IHCs is indeed carried by the BK channel.

The magnitude of the fast activating current is quantified across genotypes by comparing the peak current recorded in control external solution shortly (1 ms) after applying the test potential (Fig. 3*D*). At all test potentials, IHCs from *Slo*$^{+/-}$ had currents statistically similar to those measured in IHCs from *Slo*$^{+/+}$ mice ($p = 0.2$ at 40 mV). In contrast, IHCs from *Slo*$^{-/-}$ mice had much smaller currents than IHCs from both the *Slo*$^{+/+}$ ($p = 0.0002$ at 40 mV) and *Slo*$^{+/-}$ mice ($p = 0.00002$ at 40 mV). Specifically, at 40 mV, *Slo*$^{+/+}$ had 14 ± 1.2 nA, *Slo*$^{+/-}$ had 12 ± 1.2 nA, and *Slo*$^{-/-}$ had 60 ± 200 pA of current 1 ms after application of the test potential. The magnitude of the slowly activating current was quantified across genotypes by comparing the peak current record in the presence of 100 nM IBTX near the end of the test potential (at 19 ms; Fig. 3*E*). IHCs from all genotypes showed statistically similar magnitudes of current across test potentials ($p \geq 0.2$ at 40 mV). Specifically, at 40 mV IHCs from *Slo*$^{+/+}$ had 10 ± 1.2 nA, *Slo*$^{+/-}$ had 8.6 ± 1.8 nA, and *Slo*$^{-/-}$ had 12 ± 2.7 nA of current 19 ms after application of the test potential. These data not only confirm the absence of the BK current from *Slo*$^{-/-}$ mice but also show that the IHCs from *Slo*$^{-/-}$ mice possess no compensatory fast activating currents that could confound subsequent interpretation of the contribution of BK channels to IHC function.

Neither the BKβ1 nor BKβ4 Subunit Is Essential for the Subcellular Localization, Developmental Acquisition, or Expression of the BKα Subunit in Inner Hair Cells—Both the BKβ1 and BKβ4 subunit transcripts are expressed in IHCs during development (22) and may influence expression of the BKα subunit. The effect of the absence of these subunits on BK channel local-

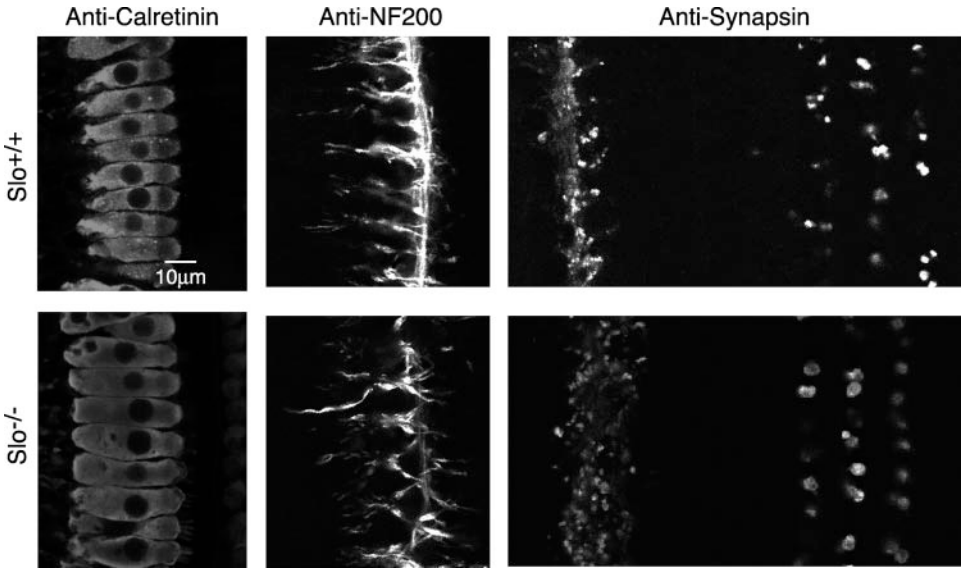

FIGURE 2. **Inner hair cells from $Slo^{-/-}$ mice have normal morphology and synaptic innervation.** Intact organs of Corti from 8-week-old $Slo^{+/+}$ and $Slo^{-/-}$ mice were immunostained as described under "Experimental Procedures." The morphology of the IHCs and their synaptic innervation was assessed by immunostaining with antibodies against the hair cell marker calretinin, the afferent fiber marker NF200, and the efferent presynapse marker synapsin. Immunostaining with a monoclonal calretinin antibody reveals similar morphology of the IHCs from both $Slo^{+/+}$ and $Slo^{-/-}$ mice. Labeling with a monoclonal antibody against NF200 or a polyclonal antibody against synapsin shows no gross differences between $Slo^{+/+}$ and $Slo^{-/-}$ mice in the organization or density of the synaptic innervation to the hair cells.

ization, developmental acquisition, and expression was studied in IHCs from 3-week-old $\beta1/4^{-/-}$ mice. Immunostaining with antibodies against the BK channel was used to determine the subcellular localization of the channel and assess its developmental acquisition. Fig. 4*A* shows IHCs double-immunostained with a monoclonal antibody against calretinin (*green*) to mark the IHC bodies and also with a polyclonal antibody against the BK channel (*red*). BK channels are indeed present in the IHCs from $\beta1/4^{-/-}$ mice and, moreover, are located near the apex of the IHCs (oriented to the *right* in Fig. 4, *A–C*), as has been previously reported in wild type mice (17, 20). Double immunostaining experiments with both a polyclonal (*green*) and monoclonal (*red*) BK channel antibody show similar patterns of staining (Fig. 4*B*). Finally, immunostaining with the polyclonal BK channel antibody reveals little immunoreactivity in mice before the onset of hearing (10 days old) and increasing immunoreactivity from just after the onset of hearing (14 days old) to the maturation of hearing (20 days old). These findings (Fig. 4*C*) are comparable with those previously reported in wild type mice (17, 20) and consistent with the observed developmental acquisition of $I_{K,f}$ (17, 19, 20).

Whole cell voltage clamp recordings were used to examine BK channel expression in 3-week-old mice. No qualitative differences were observed in the BK currents isolated from IHCs from $\beta1/4^{-/-}$ relative to wild type C57BL/6 (C57 WT) mice by subtraction of traces recorded in the presence of 100 nM IBTX in the external solution from currents recorded in control external solutions (Fig. 4*D*). The magnitude of the fast activating (predominantly BK) current is quantified across genotypes by comparing the peak current recorded in control external solution shortly (1 ms) after applying the test potential (Fig. 4*E*). No differences in the magnitude of these currents were observed across the entire range of potentials tested ($p = 0.8$ at 40 mV). IHCs from C57 WT mice had 15 ± 1.9 nA and IHCs from $\beta1/4^{-/-}$ mice had 14 ± 1.6 nA of current 1 ms after application of a 40-mV test potential. The rate of inactivation of the isolated BK currents was also examined over a range of positive test potentials (Fig. 4*F*). Again, no differences were observed between $\beta1/4^{-/-}$ and C57 WT mice ($p = 0.06–0.8$). Together, results from electrophysiology and immunostaining suggest that the BKβ1 and BKβ4 subunits play no essential role in regulating either the magnitude or apparent inactivation of the BK current expressed in IHCs or the subcellular localization or developmental acquisition of BK channels in IHCs. Finally, it has been suggested that the inactivation of BK currents isolated by subtraction is the result of series resistance errors (26). However, we find that neither series resistance errors nor potassium accumulation can account for the decay in the subtracted traces (see supplemental materials).

$Slo^{-/-}$ and $\beta1/4^{-/-}$ Mice Have Apparently Normal Inner Hair Cell Function—The normal morphology and innervation of the IHCs and the absence of the BK current or other fast activating current from IHCs suggest that $Slo^{-/-}$ mice are ideal subjects for testing the specific contribution of the BKα subunit to IHC function. IHC function was assessed by examining the ABR. Thresholds for a click (broadband) stimulus and stimuli of pure tones (8, 16, and 32 kHz) were determined for 12-week-old $Slo^{+/+}$, $Slo^{+/-}$, $Slo^{-/-}$ mice (Fig. 5*A*). Thresholds were not statistically significantly different ($p = 0.4–0.6$) between the different genotypes. Moreover, the determined thresholds were comparable with previously published values (43). These results clearly show that $Slo^{-/-}$ mice have no obvious deficits in their IHC function.

Since BK currents in IHCs have been specifically hypothesized to allow phase locking of the afferent fibers to low frequency sounds (44, 45), IHC function of $Slo^{+/+}$ and $Slo^{-/-}$ mice was also tested at low kilohertz frequencies, frequencies at which phase locking occurs. $Slo^{+/+}$ had thresholds comparable with those for higher frequencies (Fig. 5*A*). Specifically, thresholds were between 46 and 34 dB SPL in response to pure tones of 1, 2, and 4 kHz (Fig. 5*B*). Thresholds were not statistically significantly different ($p = 0.1–0.9$) for $Slo^{-/-}$ mice. These results corroborate previous examination of BKα subunit-deficient mice (24). Although these mice showed progressive hearing loss at higher frequencies, low frequency hearing (less than 10 kHz) remained normal (24). Although there were no significant differences in the hearing thresholds determined by ABR, first peak latencies were delayed in the ABRs of $Slo^{-/-}$ compared with $Slo^{+/+}$ mice. Specifically, at 16 kHz (100 dB SPL), first peak latencies were 1.33 ± 0.09 ms in $Slo^{+/+}$ mice ($n = 10$)

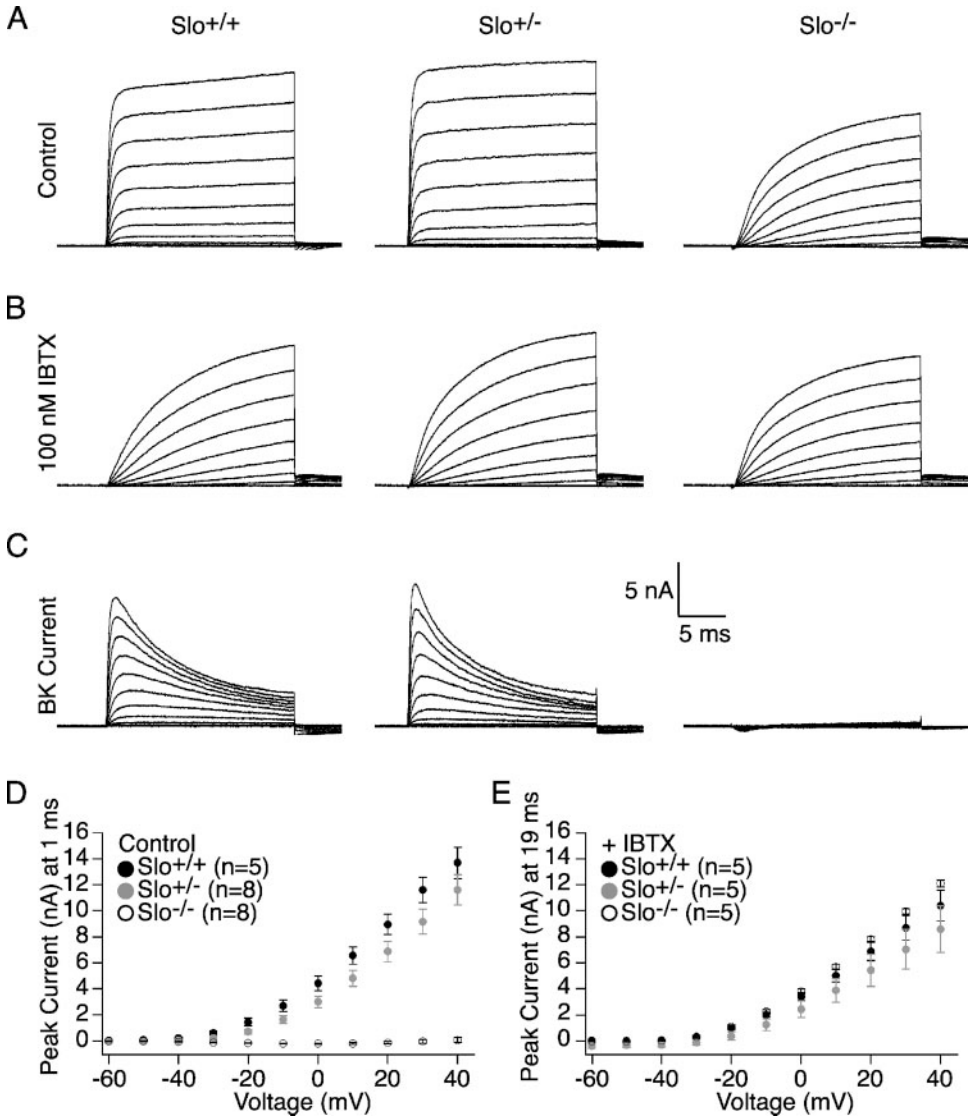

FIGURE 3. **Inner hair cells from *Slo*$^{-/-}$ mice lack the fast activating BK current and have no compensatory changes in the remaining outward currents.** Outward currents in response to depolarizations from −60 to 40 mV in 10-mV steps were recorded from IHCs from intact organs of Corti from 3-week-old *Slo*$^{+/+}$, *Slo*$^{+/-}$, and *Slo*$^{-/-}$ mice. Outward currents recorded from IHCs from *Slo*$^{+/+}$ and *Slo*$^{+/-}$ mice show a fast activating current in control solution (*A*) that can be blocked by the addition of 100 nM IBTX in the extracellular solution (*B*). In contrast, outward currents recorded from IHCs from *Slo*$^{-/-}$ mice show no fast activating current in control solution (*A*) and are not affected by application of 100 nM IBTX (*B*). Subtraction of the currents recorded in the presence of IBTX from the total currents recorded in control solution reveals the presence of BK current from IHCs from *Slo*$^{+/+}$ and *Slo*$^{+/-}$ and the absence of BK current from IHCs from *Slo*$^{-/-}$ mice (*C*). To quantitatively compare the magnitude of the fast activating current across genotypes, the magnitude of the current recorded in control solution 1 ms after application of the test potential is plotted as a function of the test potential (*D*). To quantitatively compare the magnitude of the remaining currents across genotypes, the magnitude of the current recording in the presence of 100 nM IBTX 19 ms after application of the test potential is plotted as a function of the test potential (*E*). Although *Slo*$^{-/-}$ clearly lack a fast activating potassium current, the remaining slowly activating currents appear normally expressed.

and 1.54 ± 0.09 ms in *Slo*$^{-/-}$ mice ($n = 10$; $p = 0.0001$). Similarly, at 1 kHz (100 dB SPL) first peak latencies were 1.38 ± 0.06 ms in *Slo*$^{+/+}$ mice ($n = 10$) and 1.48 ± 0.06 ms in *Slo*$^{-/-}$ mice ($n = 10$; $p = 0.001$).

Because electrophysiology verified the presence of BK currents in the IHCs from $\beta 1/4^{-/-}$ mice and because no difference in the subcellular localization or developmental acquisition of BK channels in the IHCs from $\beta 1/4^{-/-}$ mice was observed, no deficit in the IHC function of $\beta 1/4^{-/-}$ mice was expected. Functioning of the IHCs was assessed by examining the ABR of 8-week-old $\beta 1/4^{-/-}$ mice and revealed no statistically significant hearing threshold differences relative to C57 WT mice in response to either a click stimulus or stimuli of pure tones of 4, 8, 16, and 32 kHz ($p = 0.5$–1.0; Fig. 5*C*).

Slo$^{-/-}$ *and* $\beta 1/4^{-/-}$ *Mice Have Apparently Normal Outer Hair Cell Function*—Based on their sensitivity to charybdotoxin, BK currents have been identified in isolated OHCs from guinea pigs (46). Immunostaining has also indicated the presence of BK channels in OHCs (24). This same study (24) also found age-related hearing loss associated with OHC degeneration in an independently created line of mice lacking the BKα subunit. Therefore, the DPOAE was also examined to assess OHC function in 12-week-old *Slo*$^{+/+}$, *Slo*$^{+/-}$, *Slo*$^{-/-}$ mice, an age when age-related hearing loss should be evident. No differences were observed between genotypes over a range of frequencies (Fig. 6*A*).

The DPOAE was also examined to assess OHC function in 8-week-old $\beta 1/4^{-/-}$ mice (Fig. 6*B*). Again, no differences in the magnitudes of the DPOAEs were observed between $\beta 1/4^{-/-}$ and C57 WT mice over a range of frequencies. These results confirm previous observations of no OHC deficit in $\beta 1^{-/-}$ (24) and additionally show that the BKβ4 subunit is not essential for OHC function.

Regulation of Other Gene Products Does Not Compensate for the Loss of the BKα *Subunit in Slo*$^{-/-}$ *Mice*—Although electrophysiology suggested that IHCs from *Slo*$^{-/-}$ mice do not express a compensatory fast activating current, the lack of observable hearing deficit in *Slo*$^{-/-}$ mice led us to suspect that other gene products not electrophysiologically detectable might compensate for the loss of the BKα subunit. Indeed, acute blockade of the BKα subunit by perfusion of the BK channel blocker iberiotoxin into the guinea pig cochlea reduces the auditory nerve compound action potential (21), suggesting that compensatory mechanisms may be responsible for the normal hearing we observe in mice genetically designed to lack the BKα subunit at all developmental stages. Moreover, this compensation could occur in cells of the cochlea other than the IHCs. In fact, previous exam-

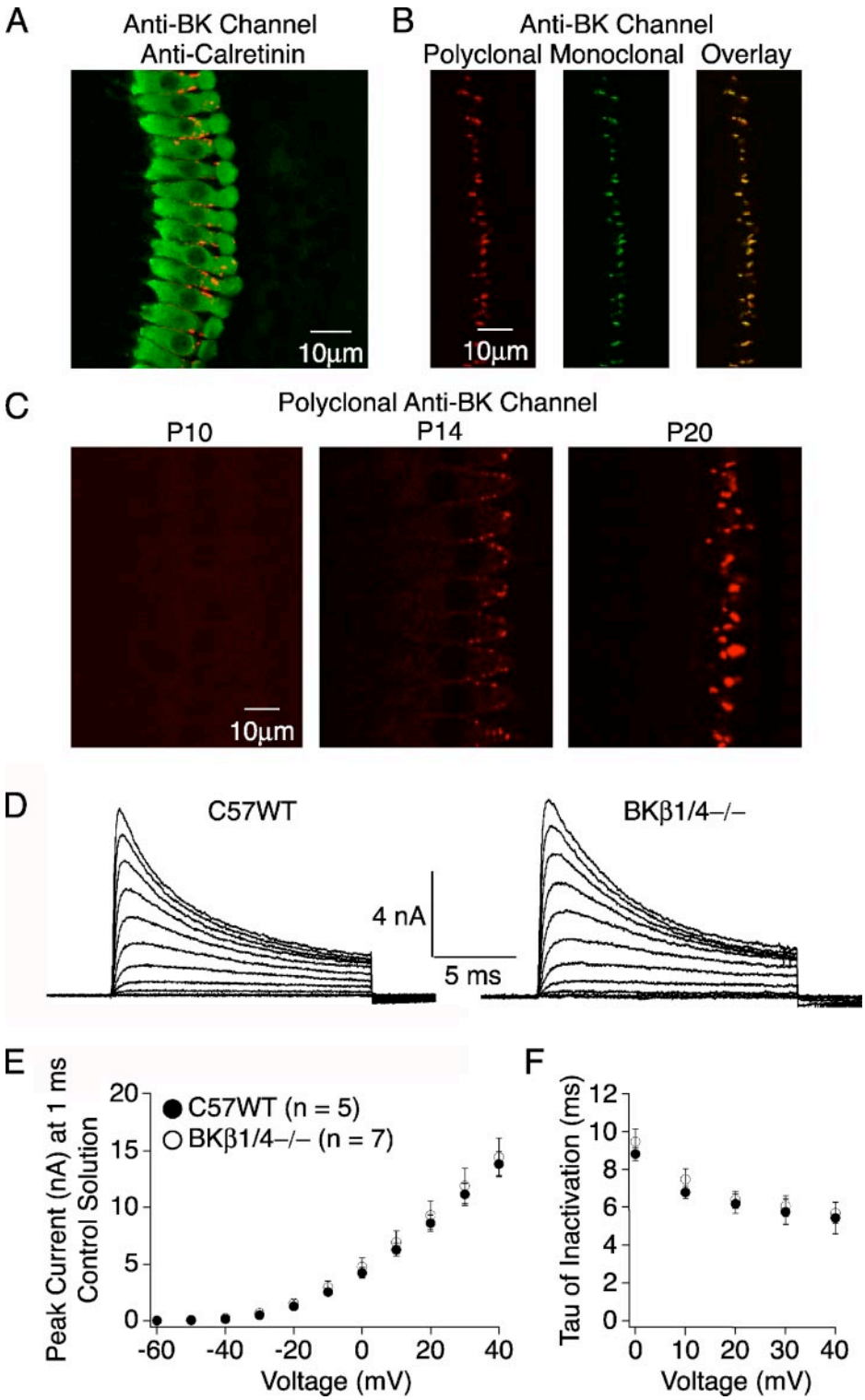

FIGURE 4. **Neither the BKβ1 nor BKβ4 subunit is essential for the subcellular localization, developmental acquisition, or expression of the BKα subunit in inner hair cells.** To assess the subcellular localization and developmental acquisition of BK channels in $\beta1/4^{-/-}$ mice, intact organs of Corti from 3-week-old $\beta1/4^{-/-}$ mice were immunostained as described under "Experimental Procedures." Immunostaining with a monoclonal calretinin antibody (*green*) and polyclonal BK channel antibody (*red*) shows punctate staining for BK channels near the apex of the IHCs (*A*). Moreover, the monoclonal BK channel antibody recognizes the same protein as the polyclonal antibody as evidenced by colocalized immunoreactivity in samples immunostained with both the polyclonal (*green*) and monoclonal (*red*) BK channel antibodies (*B*). Finally, immunostaining with a polyclonal BK channel antibody shows little immunoreactivity in IHCs from P10 mice with increasing immunoreactivity from just after the onset (P14) to the maturation (P20) of hearing (*C*), indicating that $\beta1/4^{-/-}$ mice show no developmental delay in the acquisition of BK channels. BK currents were isolated from the IHCs of 3-week-old $\beta1/4^{-/-}$ or C57 WT mice by subtracting currents recording in response to depolarizations from −60 to 40 mV in 10-mV steps from currents similarly recorded in the presence of 100 nM IBTX in the external solution (*D*). The contribution of the fast activating component was quantified by comparing the peak current recorded in control external solution shortly (1 ms) after applying the test potential. No differences in current magnitude were observed between the two genotypes (*E*). The voltage dependence of inactivation of the BK current is shown over a range of positive test potentials. No differences in the rates were observed between the two genotypes (*F*).

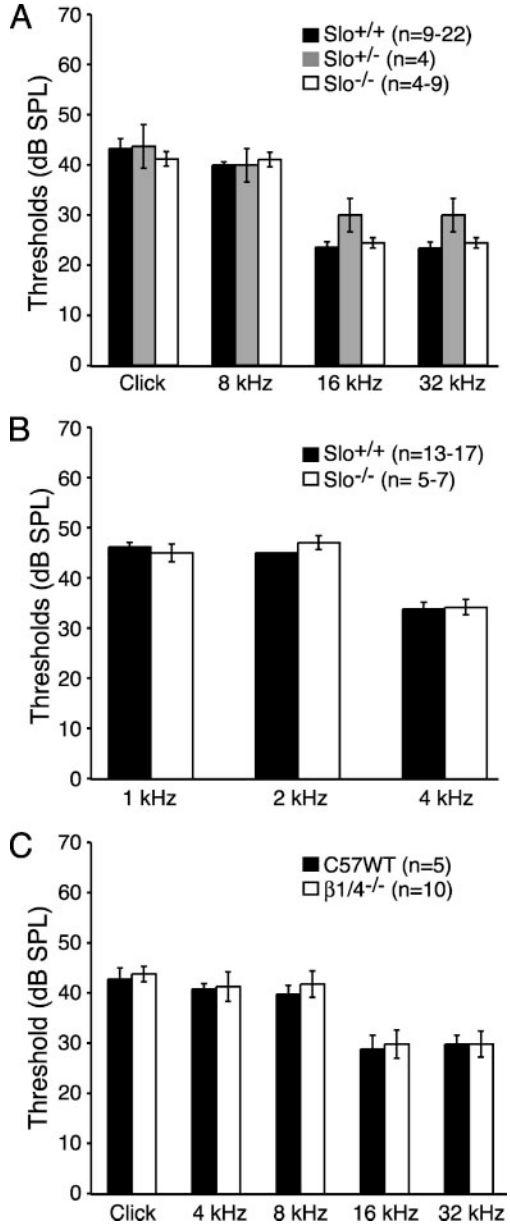

FIGURE 5. **$Slo^{-/-}$ and $\beta 1/4^{-/-}$ mice have normal inner hair cell function.** Function of the IHCs was assessed by examining the auditory brainstem responses to either a click (broadband) stimulus or stimuli of pure tones. Thresholds were not statistically significantly different between 12-week-old $Slo^{+/+}$, $Slo^{+/-}$, and $Slo^{-/-}$ mice for high frequencies (*A*), 12-week-old $Slo^{+/+}$ and $Slo^{-/-}$ mice for lower frequencies (*B*), or 8-week-old $\beta 1/4^{-/-}$ and C57 WT mice for a range of frequencies (*C*).

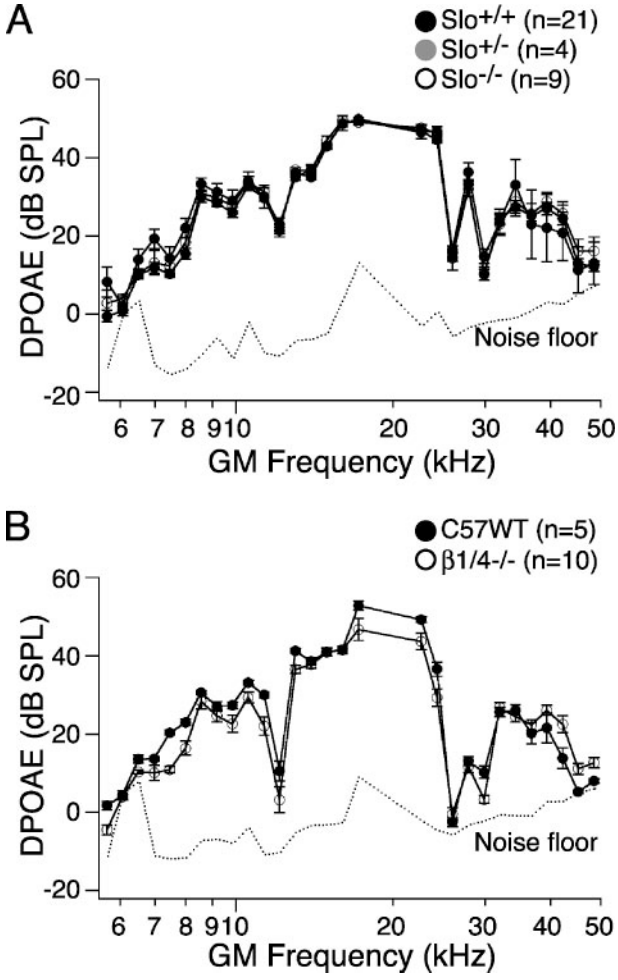

FIGURE 6. **$Slo^{-/-}$ and $\beta 1/4^{-/-}$ mice have normal outer hair cell function.** The function of the OHCs was assessed by examining the magnitude of the distortion product otoacoustic emission. No differences were observed between either 12-week-old $Slo^{+/+}$, $Slo^{+/-}$, and $Slo^{-/-}$ mice (*A*) or 8-week-old $\beta 1/4^{-/-}$ and C57 WT mice (*B*) over a range of geometric mean (*GM*) frequencies.

ination of an independently generated line of mice lacking the BKα subunit found an age-related loss of the KCNQ4 ion channel in OHCs (24).

To identify transcripts in the cochlea that might change their expression in response to the loss of the BKα subunit, DNA microarrays were used to compare gene expression differences in $Slo^{+/+}$ and $Slo^{-/-}$ mice. Three separate microarray experiments were performed: two experiments using two rounds of RNA amplification to compare expression differences between the cochleae from $Slo^{+/+}$ and $Slo^{-/-}$ mice and one experiment using a single round of RNA amplification to compare expression differences between the cochleae and cerebellum from $Slo^{+/+}$ mice and the cochleae from $Slo^{-/-}$ mice. Table 1 shows that in our experiments, transcripts known to be enriched in the cochlea (47–50) are detected as 2-fold or more enriched in the cochlea in comparison with the cerebellum (both from $Slo^{+/+}$ mice). These data indicate that microarray analyses can indeed detect expression differences in the cochlea.

To determine whether other gene products compensate for the loss of the BKα subunit, expression differences across the entire transcriptome between tissues from $Slo^{+/+}$ and $Slo^{-/-}$ mice were examined as described previously (31). Across the entire transcriptome, expression differences between the cochleae from $Slo^{+/+}$ and $Slo^{-/-}$ mice (Fig. 7*A*, *black symbols*) were highly correlated ($R^2 = 0.99$). In contrast, across the entire transcriptome, comparison of the expression differences between the cochleae and cerebellum from $Slo^{+/+}$ mice (Fig. 7*A*, *gray symbols*) revealed a much weaker relationship ($R^2 = 0.59$), despite the fact that these RNA samples were isolated from the same set of animals. Likewise, comparison of cochlea samples prepared with one round of RNA amplification with samples prepared with two rounds of amplification, revealed a weaker relationship ($R^2 \approx 0.76$) than when comparing cochlea

TABLE 1

Transcripts detected as enriched in the cochlea compared to cerebellum from *Slo*$^{+/+}$ mice

Numerous cochlea-specific transcripts are found to be enriched (greater than 2-fold) in the cochlea compared with the cerebellum from *Slo*$^{+/+}$ mice, validating the utility of microarray experiments to detect differences in transcript expression.

Transcript	Protein	Enrichment	GenBank™ ID	Probe ID
		-fold		
Apod	Apolipoprotein D	5	NM_007470.1	1416371_at
Cldn9	Claudin 9	4	NM_020293.1	1450524_at
Organ of Corti 10 kDa	Protein	115	AY078071.1	1426193_at
Otoa	Otoancorin	2	AY055122.1	1428037_at
Otog	Otogelin	4	NM_013624.1	1420797_at
S100a1	S100 calcium-binding protein A1	5	BC005590.1	1417421_at
S100a6	S100 calcium-binding protein A6 (calcyclin)	4	NM_011313.1	1421375_a_at
S100a8	S100 calcium-binding protein A8 (calgranulin A)	135	NM_013650.1	1419394_s_at
S100a9	S100 calcium-binding protein A9 (calgranulin B)	133	NM_009114.1	1448756_at
S100a10	S100 calcium-binding protein A10 (calpactin)	5	AV295650	1456642_x_at
S100a11	S100 calcium-binding protein A11 (calgizzarin)	11	NM_009115.1	1460351_at
S100a13	S100 calcium-binding protein A1	5	NM_009113.1	1418704_at
S100b	S100 protein β polypeptide	3	NM_009115.1	1419383_at

samples prepared with the same amplification scheme ($R^2 \approx 0.98$). These data indicate that comparisons across tissues or across amplification schemes yield a much larger change in the population of transcripts than does comparison across cochlea from *Slo*$^{+/+}$ or *Slo*$^{-/-}$ mice. Thus, if loss of the BKα subunit causes a change in the population of transcripts in the cochlea, this change is much smaller than the change caused by comparing cochlea tissue with another tissue or by using different RNA amplification schemes.

Although the global change in the cochlear transcriptome caused by loss of the BKα subunit appears to be small, a handful of important genes may change in ways that could compensate for the loss of the BKα subunit. In particular, other channels or transporters would be most likely to compensate for the loss of the BKα subunit. To address this possibility, expression differences in transcripts expressed in the cochleae from *Slo*$^{+/+}$ or *Slo*$^{-/-}$ mice that had the phrase "channel" (Fig. 7*B*, *black symbols*) or "transporter" (Fig. 7*B*, *gray symbols*) in the annotations provided by Affymetrix (see "Experimental Procedures") were compared. A striking correspondence for this subset of transcripts ($R^2 = 0.99$ for channels; $R^2 = 0.98$ for transporters) was observed, suggesting that there is no transcriptional compensation in other known channels or transporters that could explain the normal cochlear function observed in the *Slo*$^{-/-}$ mice.

Finally, in all three experiments, querying across the entire cochlear transcriptome revealed only a single transcript, eosinophil-associated ribonuclease 3 (*Ear3*; GenBank™ number NM_017388.1; Affymetrix Probe ID 1422412_x_at), that changes expression levels by at least 2-fold in at least two of three experiments between cochleae from *Slo*$^{+/+}$ and *Slo*$^{-/-}$ mice. The levels of this transcript were reduced (~0.5-fold) in two of the experiments and increased (~1.5-fold) in the third experiment. Because differences in transcript expression caused by loss of the BKα subunit would exhibit a consistent direction of change across experiments, changes in the opposite directions observed for *Ear3* probably reflect random biological noise.

Slo$^{-/-}$ *Mice Are Resistant to Noise-induced Hearing Loss*—The lack of observable hearing deficit in *Slo*$^{-/-}$ inbred on the FVB strain and the previously reported progressive hearing loss observed in mice lacking the BKα subunit inbred on the C57BL/6 strain (24) suggested that BK channels may be required only under extreme levels of hair cell activity and serve to protect or maintain normal hearing. To test this hypothesis, 8-week-old *Slo*$^{+/+}$ and *Slo*$^{-/-}$ mice were exposed to 1 h of 105-dB SPL sound stimulus. TSs were determined for *Slo*$^{+/+}$ and *Slo*$^{-/-}$ mice by comparing the ABRs and DPOAEs measured 5 days after exposure to their prenoise-exposed values. Although both groups of mice were temporarily deafened by the noise stimulus (had ABR thresholds greater than 100 dB SPL measured immediately after noise exposure; data not shown), *Slo*$^{-/-}$ showed significantly reduced TSs by their ABR measurements ($p = 0.005–0.02$) over a range of frequencies (Fig. 8*A*). Average TSs measured for the DPOAE were also less for *Slo*$^{-/-}$ than *Slo*$^{+/+}$ mice, although this difference was not statistically significantly different (Fig. 8*B*). 20 days following the original noise exposure, organs of Corti from noise-exposed mice were examined to identify changes in morphology that might underlie the differences in sensitivity to NIHL (Fig. 8*C*). Hair cell morphology and afferent innervation were examined by immunostaining against calretinin (*red*) and NF200 (*blue*), respectively. Actin-enriched stereocilia were examined by labeling the same samples with fluorescein isothiocyanate-conjugated phalloidin (*green*). Fig. 8*C* shows three-dimensional images reconstructed from stacks of confocal micrographs. No consistent differences in the morphology of the IHCs were observed between the two genotypes.

DISCUSSION

The ability to manipulate gene expression in the mouse has made it a prominent model for studying the molecular mechanisms of hearing. We examined mice lacking the BKα (*Slo*$^{-/-}$) and also the BKβ1 and BKβ4 (β1/4$^{-/-}$) subunits to examine their contribution to mammalian cochlear function. Our findings corroborate previous reports of normal hearing in β1$^{-/-}$ mice and additionally show that the BKβ4 subunit is not essential for normal cochlear function. BK currents isolated from IHCs from β1/4$^{-/-}$ mice appear to inactivate, a property not explained by potassium accumulation artifacts or series resistance errors. Two additional β subunits, BKβ2 and β3, have been cloned and are known to cause inactivation of BK currents (11, 14, 15, 51). Although our array data suggest the BKβ2 subunit is expressed in the mouse cochlea (data not shown), the

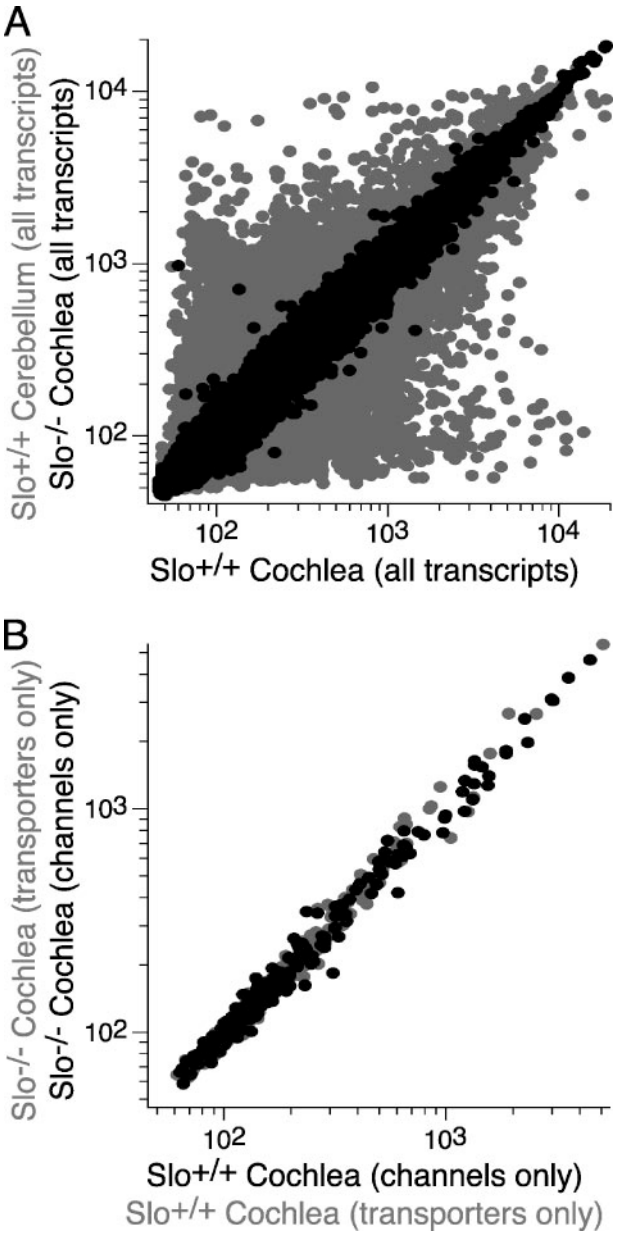

FIGURE 7. **Regulation of other gene products does not compensate for the loss of the BKα subunit in *Slo*$^{-/-}$ mice.** To identify transcripts in the cochlea that might change their expression in response to the loss of the BKα subunit, DNA microarrays were used to compare gene expression in cochleae from 8-week-old *Slo*$^{+/+}$ and *Slo*$^{-/-}$ mice and also in comparison with the cerebellum from *Slo*$^{+/+}$ mice. Comparison of the relative expression of all transcripts on the microarray from the cochleae from *Slo*$^{-/-}$ or the cerebellum from *Slo*$^{+/+}$ mice relative to cochleae from *Slo*$^{+/+}$ mice illustrates that microarray experiments are able to detect tissue-specific differences in transcript expression and yet detect few differences between the cochleae from *Slo*$^{-/-}$ and *Slo*$^{+/+}$ mice (*A*). Comparison of transcripts that specifically encode channels or transporters reveals few differences in transcript expression levels in the cochleae from *Slo*$^{-/-}$ and *Slo*$^{+/+}$ mice (*B*).

presence of these subunits in mouse IHCs is not known. An antibody against the BKβ2 subunit has recently become available and could be used to determine its expression in hair cells. Generation of transgenic animals deficient in the BKβ2 subunit would be ideal for determining whether this subunit regulates BK currents in IHCs and contributes to cochlear function *in vivo*.

Immunostaining indicated normal architecture of the hair cells in *Slo*$^{-/-}$ mice, although very subtle differences may be revealed by electrophysiology (35) or ultrastructural analysis. Immunostaining also revealed the absence of BK channels from the IHCs in *Slo*$^{-/-}$ mice. Whole-cell patch clamp recordings of IHCs from *Slo*$^{-/-}$ mice verified the absence of a fast activating potassium current. Similarly, other researchers have found negligible currents in IHCs from mice lacking the BKα subunit when recording in conditions that isolate only BK currents (26, 45). These findings provide further evidence that $I_{K,f}$ is mediated by the BK channel and, importantly, show that IHCs from *Slo*$^{-/-}$ mice do not possess another compensatory fast activating outward current. These experiments suggest that *Slo*$^{-/-}$ mice are ideal subjects for testing the specific contribution of the BKα subunit to mammalian hair cell function. Examination of the cochlear function of *Slo*$^{-/-}$ mice by measurement of the ABRs and DPOAEs revealed two startling findings: 1) no essential contribution of the BKα subunit to normal hearing and 2) increased resistance to or enhanced recovery from NIHL in the absence of the BKα subunit.

Because our findings contrasted with previous results reporting progressive hearing loss in mice lacking the BKα subunit (24), we were concerned that the normal cochlear function of *Slo*$^{-/-}$ mice could be explained by differences in the cells tested by each assay or by transcriptional compensation. First, ABRs measure IHC function over a range of sound frequencies (1–32 kHz in our experiments), whereas patch clamp recordings of IHCs are restricted to cells in the apical turn responsible for transducing low frequencies. However, physiological characterization of the frequency-place map in the mouse cochlea (52) suggests that the IHCs we recorded from (1 mm from the most apical end) respond to sound frequencies of 8 kHz and, thus, are well within the range of frequencies assessed by ABRs. Second, the recording temperature could affect the presence of compensatory currents in IHCs. In our experiments, patch clamp recordings were performed at room temperature, whereas ABRs were measured at physiological temperature. However, patch clamp experiments have been performed at both room and physiological temperature in mammalian IHCs (18, 19, 40) and indicate that compensatory currents do not appear at higher temperatures. Third, the age of the mouse from which the IHCs were isolated could affect interpretation of our results. Patch clamp recordings of IHCs become more difficult in older animals, restricting our recordings to IHCs from 3-week-old mice. In contrast, to test for progressive age-related hearing loss, auditory thresholds were assessed in 12-week-old mice. Therefore, *Slo*$^{-/-}$ mice may have hearing deficits at younger ages that become developmentally compensated. However, these results would contradict previous observations of normal hearing in mice lacking the BKα subunit at younger ages with progressive impairment at older ages (24). Furthermore, we found that the *Slo*$^{-/-}$ mice showed normal sound-evoked startle responses at the expected age for the onset of hearing (~2 weeks), suggesting no gross delay in the maturation of hearing in *Slo*$^{-/-}$ mice (data not shown). Finally, analysis of gene expression microarrays detected no compensatory differences in channel or transporter transcript expression (at ratios of less than 0.5 or greater than 2.0) in the entire cochlea of *Slo*$^{-/-}$ mice that could explain their normal cochlear function. Although

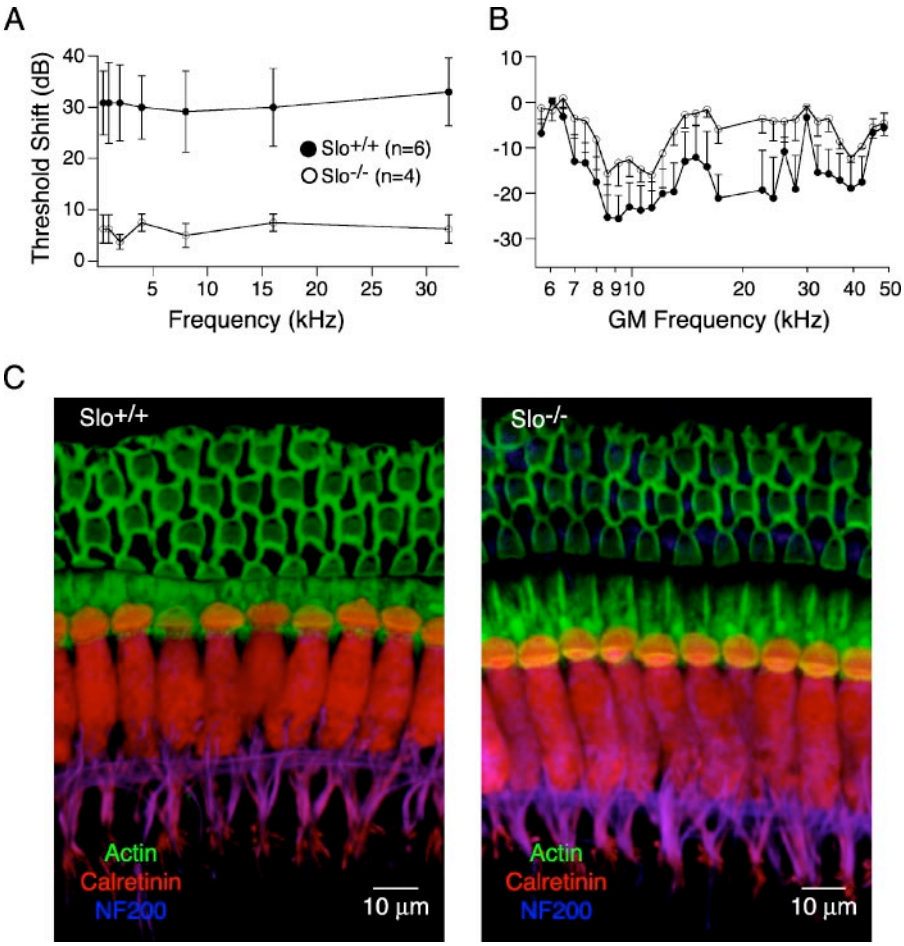

FIGURE 8. **Slo$^{-/-}$ mice show increased resistance to noise-induced hearing loss.** 8-Week-old *Slo*$^{+/+}$ and *Slo*$^{-/-}$ mice were exposed to 1 h of 105 dB SPL OBN with a center frequency of 10 kHz and a bandwidth from 8 to 16 kHz as described under "Experimental Procedures." Threshold shifts (TSs) were determined 5 days later. *Slo*$^{-/-}$ showed significantly reduced TSs by their ABR measurements ($p = 0.005–0.02$) over a range of frequencies (*A*). Average TSs measured for the DPOAE were also less for *Slo*$^{-/-}$ than *Slo*$^{+/+}$ mice, although this difference was not statistically significantly different across GM frequencies examined (*B*). Three-dimensional reconstructions of immunostained IHCs from *Slo*$^{+/+}$ and *Slo*$^{-/-}$ mice 25 days after the original noise exposure were generated from stacks of confocal micrographs as described under "Experimental Procedures" (*C*). IHCs were triple-stained with a polyclonal calretinin antibody (*red*), monoclonal NF200 antibody (isotype IgG_1; *cyan*), to stain afferent nerve fibers that contact the IHCs, and a fluorescein isothiocyanate-conjugated phalloidin to label actin (*green*). Reconstructions reveal no consistent morphological differences between IHCs from noise-exposed *Slo*$^{+/+}$ and *Slo*$^{-/-}$ mice.

compensation may not occur at the level of transcription, we were able to detect tissue-specific differences in gene expression and still found no reproducible differences in transcript expression between cochleae from *Slo*$^{+/+}$ and *Slo*$^{-/-}$ mice. The results of our microarray experiments corroborate findings in other tissues (31) and are in agreement with the previous observation that calcium and KCNQ current expression in IHCs are indistinguishable between wild type and BKα subunit-deficient mice (45).

Because we found no evidence suggesting that the normal cochlear function of *Slo*$^{-/-}$ mice was caused by differences in the populations of cells assayed or transcriptional compensation, we suspected that our results differed from those published previously (24) because of the strains of mice used to inbreed the two transgenic lines. The strain (C57BL/6) used to inbreed the mice of the previous study shows age-related hearing loss due to expression of the age-related hearing loss gene (53–55) and also greater susceptibility to noise-induced hearing loss (56). The strain (FVB/NJ) used to inbreed the mice in our experiments shows no age-dependent change in auditory thresholds (as assessed by ABR (43) or DPOAE levels (29)). Since loss of the BKα subunit appeared to accelerate hearing loss in a strain (C57BL/6) already predisposed for age-related hearing loss and NIHL, we hypothesized that BK channels are required only under extreme levels of hair cell activity and serve to protect or maintain normal hearing. Therefore, we tested *Slo*$^{+/+}$ and *Slo*$^{-/-}$ mice for their sensitivity to NIHL 5 days following noise exposure. In contrast to expectation, we found that *Slo*$^{-/-}$ mice were more resistant to NIHL than *Slo*$^{+/+}$ mice. Although longer time points (greater than 2 weeks) should be examined to determine the permanent threshold shifts, we found that average TSs were reduced for both ABRs and DPOAEs, suggesting that *Slo*$^{-/-}$ mice show reduced sensitivity to or greater recovery from NIHL. Interestingly, TSs were only significantly reduced for thresholds measured by ABRs, suggesting that IHCs may be particularly protected by the absence of the BKα subunit. Differences in TSs may also arise from differences in the afferent (45) or efferent excitability.

A number of mechanisms could be considered to explain the surprising finding that the absence of the BKα subunit confers resistance to NIHL. First, differences in the intrinsic excitability of the IHCs from *Slo*$^{+/+}$ and *Slo*$^{-/-}$ mice could affect their susceptibility to NIHL. However, the loss of a hyperpolarizing current would be expected to make IHCs from *Slo*$^{-/-}$ mice more excitable, rendering the primary afferents more susceptible to glutamate excitotoxicity and subsequent NIHL. Second, noise trauma is associated with reduced cochlear blood flow (57). Vascular differences between *Slo*$^{+/+}$ and *Slo*$^{-/-}$ mice could affect their sensitivities to NIHL. However, mice deficient for the BKα subunit are hypertensive (58) and, thus, more likely to have reduced blood flow in the microcirculation of the cochlea. Third, NIHL is known to be associated with oxidative stress, caspase activation, and apoptosis of IHCs (57, 59). Although not specifically shown in the cochlea, excessive potassium efflux is an essential mediator of early apoptotic cell shrinkage (60, 61), and oxidation has been shown to enhance BK channel activity (62). Therefore, the absence of the BKα subunit may prevent a noise-induced apoptotic potassium efflux. Indeed,

blockade of BK currents by IBTX significantly reduces potassium accumulation on the external IHC membrane (see supplemental materials). Although immunostaining revealed no signs of increased IHC shrinkage in apical turns from $Slo^{+/+}$ and $Slo^{-/-}$ mice, hair cells basal to the tonotopic site of the exposed noise frequency are known to be more susceptible to noise-induced damage (63). Thus, future experiments should investigate pathological differences in basal turns of the cochlea. Finally, noise-induced damage in the cochlea has been documented in detail in CBA mice and is known to affect multiple cell types (63). The loss of the BKα subunit from any of these cell types, some of which are known to express the BKα subunit (spiral ganglion cells (22)) or have altered excitability in the absence of the BKα subunit (primary afferents (45)), could prevent noise-induced damage and should be investigated further.

Although thresholds determined from ABR and DPOAE suggest normal cochlear functioning in mice lacking the BKα, β1, and β4 subunits, it would be surprising if BK channels play no role in normal mammalian hearing. Our experiments cannot exclude changes in the response properties of auditory nerve fibers or subsequent behavioral changes in sound localization or other timing-dependent tasks. In fact, we did observe an increase in the first peak latency in the ABRs of $Slo^{-/-}$ mice compared with $Slo^{+/+}$ mice. The first peak represents transmission across the IHC-afferent dendrite synapse. This delayed latency is consistent with previous observations of a larger IHC membrane time constant observed previously in BK channel-deficient mice (45). This previous study also used auditory nerve recordings to show that BK channel-deficient mice have deteriorated precision of spike timing (45). Nonetheless, the results of our experiments suggest that overall BK channels play a less obvious role in normal mammalian cochlear function than predicted from the nonmammalian cochlea. Although more extensive characterization of the sensitivity of BK-deficient mice to NIHL needs to be performed, the initial observation of increased resistance to NIHL in the absence of BK channels and the lack of observable transcriptional compensation suggest that BK channels play a direct role in mediating NIHL. Indeed, characterization of BKα subunit-deficient mice (this study) (45) suggests that noise-induced pathology of the cochlea may be triggered not only by the intensity but also the temporal coding of sound. Therefore, BK channels should be considered an important target in the study and prevention of NIHL.

Acknowledgments—We thank Paul A. Fuchs and Elisabeth Glowatzki for critically reviewing the manuscript and Brad J. May for helpful discussions. We also thank James S. Trimmer for technical training and assistance with experimental design and interpretation. We greatly appreciate the technical assistance of Jerel Garcia and Tonghui Xu for measuring the auditory brainstem responses and distortion product otoacoustic emissions and Elizabeth Zuo for processing the microarrays.

REFERENCES

1. Hu, H., Shao, L. R., Chavoshy, S., Gu, N., Trieb, M., Behrens, R., Laake, P., Pongs, O., Knaus, H. G., Ottersen, O. P., and Storm, J. F. (2001) *J. Neurosci.* **21,** 9585–9597
2. Pattillo, J. M., Yazejian, B., DiGregorio, D. A., Vergara, J. L., Grinnell, A. D., and Meriney, S. D. (2001) *Neuroscience* **102,** 229–240
3. Shao, L. R., Halvorsrud, R., Borg-Graham, L., and Storm, J. F. (1999) *J. Physiol.* **521,** 135–146
4. Nelson, A. B., Krispel, C. M., Sekirnjak, C., and du Lac, S. (2003) *Neuron* **40,** 609–620
5. Solaro, C. R., Prakriya, M., Ding, J. P., and Lingle, C. J. (1995) *J. Neurosci.* **15,** 6110–6123
6. Brenner, R., Perez, G. J., Bonev, A. D., Eckman, D. M., Kosek, J. C., Wiler, S. W., Patterson, A. J., Nelson, M. T., and Aldrich, R. W. (2000) *Nature* **407,** 870–876
7. Meredith, A. L., Thorneloe, K. S., Werner, M. E., Nelson, M. T., and Aldrich, R. W. (2004) *J. Biol. Chem.* **279,** 36746–36752
8. Werner, M. E., Zvara, P., Meredith, A. L., Aldrich, R. W., and Nelson, M. T. (2005) *J. Physiol.* **567,** 545–556
9. Fettiplace, R., and Fuchs, P. A. (1999) *Annu. Rev. Physiol.* **61,** 809–834
10. Shen, K. Z., Lagrutta, A., Davies, N. W., Standen, N. B., Adelman, J. P., and North, R. A. (1994) *Pflugers Arch.* **426,** 440–445
11. Brenner, R., Jegla, T. J., Wickenden, A., Liu, Y., and Aldrich, R. W. (2000) *J. Biol. Chem.* **275,** 6453–6461
12. Knaus, H. G., Folander, K., Garcia-Calvo, M., Garcia, M. L., Kaczorowski, G. J., Smith, M., and Swanson, R. (1994) *J. Biol. Chem.* **269,** 17274–17278
13. Meera, P., Wallner, M., and Toro, L. (2000) *Proc. Natl. Acad. Sci. U. S. A.* **97,** 5562–5567
14. Uebele, V. N., Lagrutta, A., Wade, T., Figueroa, D. J., Liu, Y., McKenna, E., Austin, C. P., Bennett, P. B., and Swanson, R. (2000) *J. Biol. Chem.* **275,** 23211–23218
15. Xia, X. M., Ding, J. P., and Lingle, C. J. (1999) *J. Neurosci.* **19,** 5255–5264
16. Ramanathan, K., Michael, T. H., Jiang, G. J., Hiel, H., and Fuchs, P. A. (1999) *Science* **283,** 215–217
17. Hafidi, A., Beurg, M., and Dulon, D. (2005) *Neuroscience* **130,** 475–484
18. Kros, C. J., and Crawford, A. C. (1990) *J. Physiol.* (*Lond.*) **421,** 263–291
19. Kros, C. J., Ruppersberg, J. P., and Rusch, A. (1998) *Nature* **394,** 281–284
20. Pyott, S. J., Glowatzki, E., Trimmer, J. S., and Aldrich, R. W. (2004) *J. Neurosci.* **24,** 9469–9474
21. Skinner, L. J., Enee, V., Beurg, M., Jung, H. H., Ryan, A. F., Hafidi, A., Aran, J. M., and Dulon, D. (2003) *J. Neurophysiol.* **90,** 320–332
22. Langer, P., Grunder, S., and Rusch, A. (2003) *J. Comp. Neurol.* **455,** 198–209
23. Brandle, U., Frohnmayer, S., Krieger, T., Zenner, H. P., Ruppersberg, J. P., and Maassen, M. M. (2001) *Hear. Res.* **161,** 23–28
24. Ruttiger, L., Sausbier, M., Zimmermann, U., Winter, H., Braig, C., Engel, J., Knirsch, M., Arntz, C., Langer, P., Hirt, B., Muller, M., Kopschall, I., Pfister, M., Munkner, S., Rohbock, K., Pfaff, I., Rusch, A., Ruth, P., and Knipper, M. (2004) *Proc. Natl. Acad. Sci. U. S. A.* **101,** 12922–12927
25. Marcotti, W., Johnson, S. L., and Kros, C. J. (2004) *J. Physiol.* (*Lond.*) **557,** 613–633
26. Thurm, H., Fakler, B., and Oliver, D. (2005) *J. Physiol.* (*Lond.*) **569,** 137–151
27. Rusch, A., Ng, L., Goodyear, R., Oliver, D., Lisoukov, I., Vennstrom, B., Richardson, G., Kelley, M. W., and Forrest, D. (2001) *J. Neurosci.* **21,** 9792–9800
28. Brenner, R., Chen, Q. H., Vilaythong, A., Toney, G. M., Noebels, J. L., and Aldrich, R. W. (2005) *Nat. Neurosci.* **8,** 1752–1759
29. Martin, G. K., Vazquez, A. E., Jimenez, A. M., Koivisto, D. L., Candreia, C. M., and Lonsbury-Martin, B. L. (2001) *Association for Research in Otolaryngology Abstracts*, Abstr. 21416, Association for Research in Otolaryngology, Mt. Royal, NJ
30. Jimenez, A. M., Stagner, B. B., Martin, G. K., and Lonsbury-Martin, B. L. (1999) *Hear. Res.* **138,** 91–105
31. Meredith, A. L., Wiler, S. W., Miller, B. H., Takahashi, J. S., Fodor, A. A., Ruby, N. F., and Aldrich, R. W. (2006) *Nat. Neurosci.* **9,** 1041–1049
32. Lee, M. P., Ravenel, J. D., Hu, R. J., Lustig, L. R., Tomaselli, G., Berger, R. D., Brandenburg, S. A., Litzi, T. J., Bunton, T. E., Limb, C., Francis, H., Gorelikow, M., Gu, H., Washington, K., Argani, P., Goldenring, J. R., Coffey, R. J., and Feinberg, A. P. (2000) *J. Clin. Invest.* **106,** 1447–1455
33. Platzer, J., Engel, J., Schrott-Fischer, A., Stephan, K., Bova, S., Chen, H., Zheng, H., and Striessnig, J. (2000) *Cell* **102,** 89–97

34. Vetter, D. E., Mann, J. R., Wangemann, P., Liu, J., McLaughlin, K. J., Lesage, F., Marcus, D. C., Lazdunski, M., Heinemann, S. F., and Barhanin, J. (1996) *Neuron* **17,** 1251–1264
35. Brandt, A., Striessnig, J., and Moser, T. (2003) *J. Neurosci.* **23,** 10832–10840
36. Zheng, J. L., and Gao, W. Q. (1997) *J. Neurosci.* **17,** 8270–8282
37. Berglund, A. M., and Ryugo, D. K. (1991) *J. Comp. Neurol.* **306,** 393–408
38. Von Kriegstein, K., Schmitz, F., Link, E., and Sudhof, T. C. (1999) *Eur. J. Neurosci.* **11,** 1335–1348
39. Helyer, R. J., Kennedy, H. J., Davies, D., Holley, M. C., and Kros, C. J. (2005) *Audiol. Neurootol.* **10,** 22–34
40. Marcotti, W., Johnson, S. L., Holley, M. C., and Kros, C. J. (2003) *J. Physiol.* (*Lond.*) **548,** 383–400
41. Oliver, D., Knipper, M., Derst, C., and Fakler, B. (2003) *J. Neurosci.* **23,** 2141–2149
42. Galvez, A., Gimenez-Gallego, G., Reuben, J. P., Roy-Contancin, L., Feigenbaum, P., Kaczorowski, G. J., and Garcia, M. L. (1990) *J. Biol. Chem.* **265,** 11083–11090
43. Zheng, Q. Y., Johnson, K. R., and Erway, L. C. (1999) *Hear. Res.* **130,** 94–107
44. Kros, C. J. (1996) in *The Cochlea* (Dallos, P., Popper, A. N., and Fay, R. R., eds) pp. 318–385, Springer-Verlag New York Inc., New York
45. Oliver, D., Taberner, A. M., Thurm, H., Sausbier, M., Arntz, C., Ruth, P., Fakler, B., and Liberman, M. C. (2006) *J. Neurosci.* **26,** 6181–6189
46. Nenov, A. P., Norris, C., and Bobbin, R. P. (1996) *Hear. Res.* **101,** 149–172
47. Chen, Z. Y., and Corey, D. P. (2002) *J. Assoc. Res. Otolaryngol.* **3,** 140–148
48. Simmler, M. C., Cohen-Salmon, M., El-Amraoui, A., Guillaud, L., Benichou, J. C., Petit, C., and Panthier, J. J. (2000) *Nat. Genet.* **24,** 139–143
49. Morris, K. A., Snir, E., Pompeia, C., Koroleva, I. V., Kachar, B., Hayashizaki, Y., Carninci, P., Soares, M. B., and Beisel, K. W. (2005) *J. Assoc. Res. Otolaryngol.* **6,** 75–89
50. Hildebrand, M. S., de Silva, M. G., Klockars, T., Solares, C. A., Hirose, K., Smith, J. D., Patel, S. C., and Dahl, H. H. (2005) *Hear. Res.* **200,** 102–114
51. Wallner, M., Meera, P., and Toro, L. (1999) *Proc. Natl. Acad. Sci. U. S. A.* **96,** 4137–4142
52. Muller, M., von Hunerbein, K., Hoidis, S., and Smolders, J. W. (2005) *Hear. Res.* **202,** 63–73
53. Johnson, K. R., Erway, L. C., Cook, S. A., Willott, J. F., and Zheng, Q. Y. (1997) *Hear. Res.* **114,** 83–92
54. Erway, L. C., Shiau, Y. W., Davis, R. R., and Krieg, E. F. (1996) *Hear. Res.* **93,** 181–187
55. Davis, R. R., Newlander, J. K., Ling, X., Cortopassi, G. A., Krieg, E. F., and Erway, L. C. (2001) *Hear. Res.* **155,** 82–90
56. Jimenez, A. M., Stagner, B. B., Martin, G. K., and Lonsbury-Martin, B. L. (2001) *J. Assoc. Res. Otolaryngol.* **2,** 233–245
57. Henderson, D., Bielefeld, E. C., Harris, K. C., and Hu, B. H. (2006) *Ear Hear.* **27,** 1–19
58. Sausbier, M., Arntz, C., Bucurenciu, I., Zhao, H., Zhou, X. B., Sausbier, U., Feil, S., Kamm, S., Essin, K., Sailer, C. A., Abdullah, U., Krippeit-Drews, P., Feil, R., Hofmann, F., Knaus, H. G., Kenyon, C., Shipston, M. J., Storm, J. F., Neuhuber, W., Korth, M., Schubert, R., Gollasch, M., and Ruth, P. (2005) *Circulation* **112,** 60–68
59. Van De Water, T. R., Lallemend, F., Eshraghi, A. A., Ahsan, S., He, J., Guzman, J., Polak, M., Malgrange, B., Lefebvre, P. P., Staecker, H., and Balkany, T. J. (2004) *Otol. Neurotol.* **25,** 627–632
60. Yu, S. P. (2003) *Prog. Neurobiol.* **70,** 363–386
61. Remillard, C. V., and Yuan, J. X. (2004) *Am. J. Physiol.* **286,** L49–L67
62. Tang, X. D., Daggett, H., Hanner, M., Garcia, M. L., McManus, O. B., Brot, N., Weissbach, H., Heinemann, S. H., and Hoshi, T. (2001) *J. Gen. Physiol.* **117,** 253–274
63. Wang, Y., Hirose, K., and Liberman, M. C. (2002) *J. Assoc. Res. Otolaryngol.* **3,** 248–268
64. Kimitsuki, T., Kawano, K., Matsuda, K., Haruta, A., Nakajima, T., and Komune, S. (2003) *Hear. Res.* **180,** 85–90
65. Armstrong, C. E., and Roberts, W. M. (2001) *J. Physiol.* (*Lond.*) **536,** 49–65